Int J Leg Med (1994) 107:132–140

ORIGINAL ARTICLE

M. Cingolani · A. Osculati · A. Tombolini
A. Tagliabracci · C. Ghimenton · S. D. Ferrara

Morphology of sweat glands in determining time of death

Received: 8 October 1994 / Received in revised form: 28 April 1994

Abstract This study demonstrates post-mortem autolytic alterations in the skin at cellular and subcellular levels and identifies parameters which may assist in determining the time of death in the first few hours post-mortem. Serial skin samples from the ventral surface of the arm were taken at intervals of 3, 6, 9 and 12 h after death in 29 subjects of various ages, with no signs of skin disease; causes of death were various. Three types of tests were performed: cytochemical (hematoxylin-eosin and alcian-PAS), immunohistochemical (S-100, CEA, Cytokeratin, ASM) and ultrastructural (electron microscopy). Electron microscopy proved useful for identifying transformations which were found to be specific for each chronological step considered: reduction of intracellular glycogen in clear cells and reduction of secretory granules in dark cells are typcial signs of the first stage (3 h) after death; mitochondrial dilatation and rarefaction of cristae in clear and dark cells are typical of the second stage (6 h); rarefaction of microvilli in dark and clear cells is a sign of the last stage (12 h). Cytochemistry and immunohistochemistry supply useful information – not for all the chronological stage considered here, but for individual phases (3 h for hematoxylin-eosin and 6 h for alcian-PAS). However, it is particularly important to use the results from all such techniques simultaneously, so that the question of the exact time of death within the first 12 h post-mortem may be more accurately answered.

M. Cingolani · A. Osculati · A. Tombolini · A. Tagliabracci
Istituto di Medicina Legale, Università di Ancona,
Ospedale Regionale, I-60020 Ancona, Italy

C. Ghimenton
Servizio di Anatomia Patologica, Ospedale Civile Maggiore,
Verona, Italy

S. D. Ferrara (✉)
Centre of Behavioural and Forensic Toxicology,
Istituto di Medicina Legale, University of Padova,
Via Falloppio 50, I-35121 Padova, Italy

Key words Time of death · Sweat glands
Immunohistochemistry · Electron microscopy

Zusammenfassung Diese Untersuchung zeigt postmortale autolytische Veränderungen in der Haut auf zellulärer und subzellulärer Ebene und identifiziert Parameter, welche helfen können, die Zeit des Todes in den ersten Stunden postmortem zu bestimmen. Hautproben von der Beugeseite des Arms wurden, 3, 6, 9 und 12 Stunden nach dem Tode von insgesamt 29 Leichen entnommen (verschiedene Altersklassen, keine Zeichen für Hauterkrankungen, verschiedene Todesursachen). Drei Arten der Untersuchungen wurden durchgeführt: zytochemisch (Hematoxylin-Eosin and Alcian-PAS), immunhistochemisch (S-100, CEA, Cytokeratin, ASM) und ultrastrukturell (Elektronenmikroskopie). Die Elektronenmikroskopie erwies sich als nützlich für die Identifizierung von Transformationen die für jeden chronologischen Schritt spezifisch waren: Reduktion des intrazellulären Glykogens in hellen Zellen und Reduktion der sekretorischen Granula in dunklen Zellen sind typische Zeichen für die erste Phase (3 Stunden) nach dem Tode; mitochondriale Dilatation und Rarifizierung der Cristae in hellen und dunklen Zellen sind typisch für die 2. Phase (6 Stunden); Rarifizierung der Microvilli in dunklen und hellen Zellen sind typisch für die 3. Phase (9 Stunden) und Kernpyknose von dunklen und hellen Zellen ist ein Zeichen der letzten Phase (12 Stunden). Zytochemie und Immunhistochemie sorgen für eine nützliche Information – dies gilt nicht für alle chronologischen Stadien, welche hier einbezogen wurden, aber für individuelle Phasen (3 Stunden für Hematoxylin-Eosin und 6 Stunden für Alcian-PAS). Es ist jedoch besonders wichtig, die Resultate von allen solchen Techniken simultan einzubeziehen, so daß die Frage der exakten Todeszeit innerhalb der ersten 12 Stunden postmortem genauer beantwortet werden kann.

Schlüsselwörter Todeszeit · Schweißdrüsen
Immunhistochemie · Elektronenmikroskopie

Introduction

Determination of time of death and of the post-mortem interval (PMI) is one of most important tasks of the forensic pathologist [1, 2].

Janssen [3] pointed out that histology is an invaluable tool for the forensic pathologist in determining the time of death, especially time-related morphological changes of several human tissues, including skin. In particular, the author reports that intracellular glycogen deposits rapidly decrease in skin cells.

Previous studies [4, 5] show that sweat glands may be suitable structures for determining the time of death. This study aimed at investigating post-mortem autolytic alterations of the skin at cellular and subcellular levels and at identifying microscopical parameters which may assist in determining the time of death in the first 12 h post-mortem.

Of the skin glands, eccrine sweat glands are the most important because they control body temperature [6]. They are located everywhere on the body surface, particularly on the sole of the foot and palm of the hand, but are absent in some areas such as the lips, glans and clitoris [7].

The structure of eccrine sweat glands is of the tubular type [8]. The gland tubule may be divided into 2 main parts: secretory tubule and duct. The secretory tubule is not branched, has a narrow lumen, and represents almost 50% of the total gland length [8]. It is composed of 3 types of cells forming a continuous wall surrounded by a thin basal membrane [8]. The outer elements are myoepithelial cells which, with their extensions, form a basket surrounding the internal row of secretory cells. The latter differ in morphology and the chemical composition of the secretion. Because the present study concerns morphological changes in sweat gland cells occurring after death, a morphological classification is adopted here [7–9], that distinguishes 2 types of secretory elements, clear and dark cells. Table 1 summarizes the morphological characteristics of the 2 cell types in light microscopy. Electron microscopy has revealed several subcellular differences between clear and dark cells [9] (Fig. 1), summarized in Table 2. The luminal part of the secretory cell membrane has numerous microvilli. Secretory capillaries are found between the clear cells. The cell membrane forming the wall of the capillaries is rich in microvilli.

The duct is formed of 2 rows of cells. The internal cells are small and cube-shaped, with a high nucleus-cytoplasm ratio. The external cells are thin, in contact with the basal membrane, and rich in mitochondria.

Table 1 Normal morphology of sweat glands by light microscopy

Parameter	Cell type	
	Clear	Dark
Cell density	High	Low
Size	Large	Small
Shape	Truncated cone Large base in contact with myoepithelial cells and basal membrance	Truncated cone Large base in contact with gland lumen
Cytoplams	Acidophilic	Basophilic

Materials and methods

This study was carried out on skin samples from 29 corpses (17 male, 12 female) with an average age of 74 years at death (range

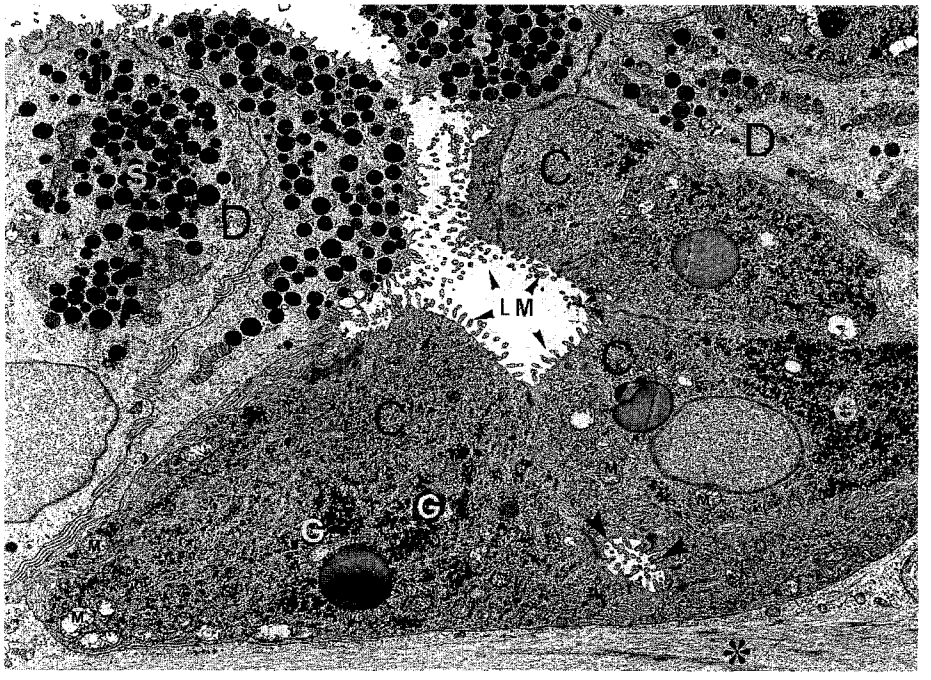

Fig. 1 Electron microscopy of normal sweat gland (× 10,000). Note lumen microvilli (*arrows*). C, clear cell; D, dark cell; G, glycogen granules; S, secretory granules; M, mitochondria; *, myoepithelial cell

Table 2 Normal morphology of sweat glands in electron microscopy

Parameter	Cell type	
	Clear	Dark
Mitochondria	Numerous	Normal
Glycogen particles	Abundant	Normal
Smooth endoplasmic reticulum	Abundant	Normal
Secretory granules	Absent	Present

54–94). In all cases death was due to natural causes (ischemic and degenerative heart disease, $n = 15$; tumours, $n = 6$; cerebral ictus, $n = 4$; diabetic coma, hepatic cirrhosis, pulmonary silicosis and pulmonary emboly, 1 each), but no subjects had any skin disease. The bodies were placed in observation rooms where the temperature and humidity were not modified artificially. Serial skin samples from the ventral surface of the arm were taken at intervals of 3, 6, 9 and 12 h after death. Traumatic changes were carefully avoided when handling the skin fragments.

Light microscopy

Samples were fixed in buffered formalin, embedded in paraffin wax, and stained with hematoxylin-eosin and alcian-PAS.

Immunohistochemistry

After double incubation with primary and secondary antibodies (ABC method; Vectorstain) [10, 11], antigen-antibody binding sites were stained using diaminobenzidine as substrate (Sigma Chemical Co., St. Louis, Mo., USA). Samples of normal biopsy skin were examined to check the validity of the method and the quality of the reagents. The following tests and antisera were applied to all samples and to controls:

S-100 Protein

S-100 is a protein controlling calcium flow through the cell membrane [10–12]. The test is based on the use of rabbit antiserum against human S-100 protein (Code Z 311, Dakopatts A/S, Glostrup, DK).

Carcinoembryonic antigen (CEA)

Carcinoembryonic Antigen is found in the apex of secretory cells, forming a continuous ring surrounding the lumen of the secretory tubule and capillaries. The test is based on the use of rabbit antiserum against human-CEA (Code A 115, Dakopatts A/S, Glostrup, DK).

Cytokeratin

This test detects antigens in tissue sections, cell preparations and cytospins. It is based on the use of mouse and rabbit antiserum against human cytokeratin protein (Code 371-5M, Ortho Diagnostic Systems, Raritan, N.J., USA).

Actin smooth muscle (ASM)

The test detects antigens in tissue sections, cell preparations and cytospins. It is based on the use of mouse and rabbit antiserum against human actin smooth muscle protein (Code 428-5M, Ortho Diagnostic Systems, Raritan, N.J., USA).

Each test was carried out taking precautions regarding storage and handling of tissues and following staining procedures in accordance with the manufacturers' instructions.

Electron microscopy

Skin samples were first fixed in a solution of Sorensen glutaraldehyde buffer (2%) at pH 7.4 and a temperature of 4° C for 4 h, and then in a solution of osmium tetroxide potassium ferrocyanide buffer (1:1:98) for 1 h at room temperature. Samples were subsequently dehydrated in ethanol solutions at increasing concentrations and embedded in Epon-Araldite (Araldite 502 kit, AR-502, Sigma Chemical Co., St. Louis, Mo., USA). The ultrathin sections obtained from the specimens were stained with a solution of lead citrate (4 mg/ml H_2O) and uranyl acetate (saturated solution in ethanol). Electron microscope observations were performed using Zeiss EM 10 equipment. Photograms at 10,000 magnification accurately revealed all selected parameters.

Results and discussion

The results of this study show that sweat gland cells undergo progressive morphological changes after death, which may be investigated at cellular level by light microscopy or immunohistochemistry, or at subcellular level by electron microscopy. The results obtained and relative interpretations for each of the techniques used are reported below.

Light microscopy

The hematoxylin-eosin method stains all cell elements of glands and reveals the progressive retraction of the cytoplasm, a sign of cell degeneration. Three hours after death no morphological changes were present (Fig. 2 B), and the morphological equivalent of cell degeneration was the presence of empty cytoplasmic vacuoles in the gland cells 6 h after death (Fig. 2 C) which increased in number 9 and 12 h after death (Fig. 2 D). Therefore, although this method may reveal the time of death after 6 hours, it cannot do so any earlier. Another limitation is that differential diagnosis between 9 and 12 h after death is difficult and depends on the examiner's subjective evaluation. However, the advantage of this method is that the forensic pathologist may obtain an approximate indication of the time of death with a simple, rapid and cheap technique.

The alcian-PAS method stains the cytoplasm of secretory tubule cells, apex of duct cells, and basal membrane. Glycogen particles are stained purple (Fig. 3 A). The variations in colour intensity with time are reported in Table 3 and shown in Fig. 3 B. Because the glycogen particles characteristically disappear and the secretory tubule cells progressively lose their PAS positivity within 6 h (Fig. 1B), this method reveals morphological alterations taking place 0–6 h after death

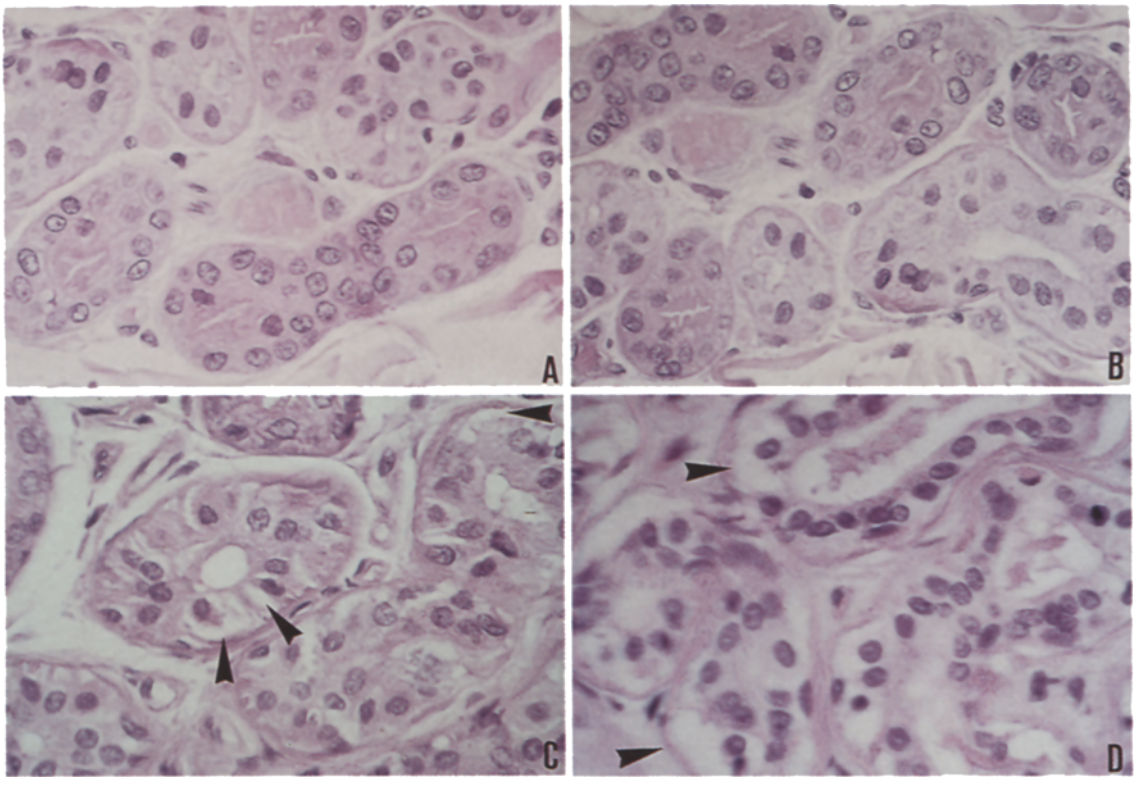

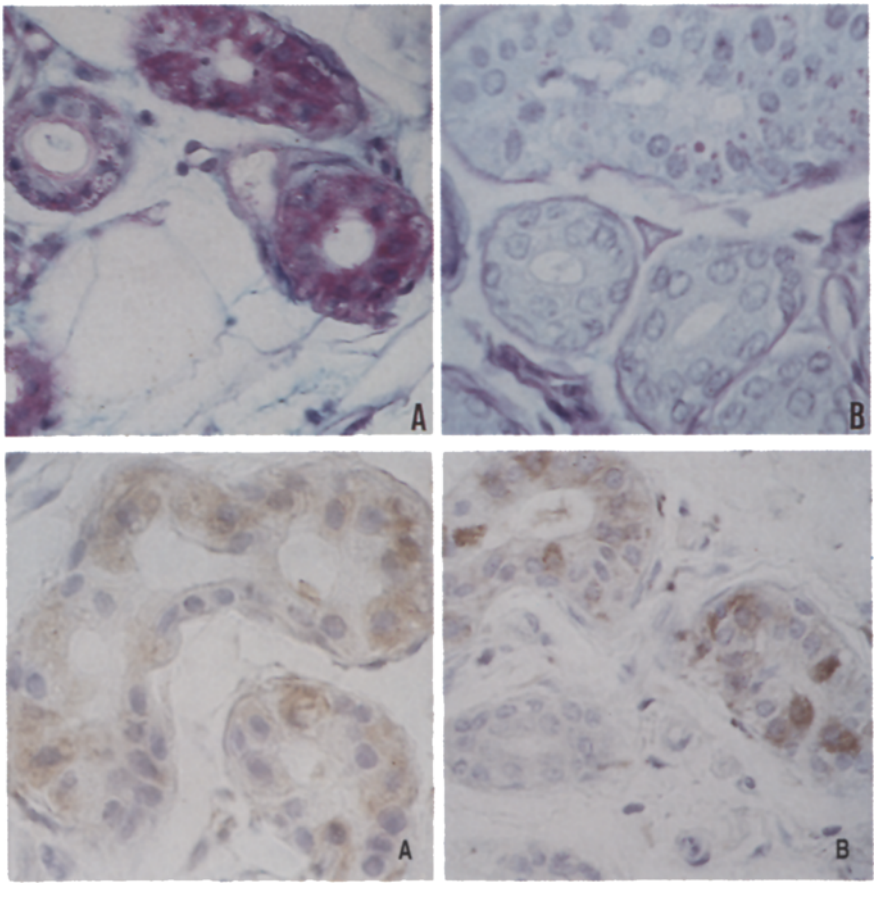

Fig. 2 A–D Secretory cells (hematoxylin-eosin × 400). **A** (normal skin); **B** (3 h after death): no changes; **C** (6 h after death): note early presence of cytoplasmic vacuoles (*arrows*). **D** (9 h after death): note increase in cytoplasmic vacuoles (*arrows*)

Fig. 3 A, B Secretory cells (Alcian-PAS × 400). **A** (normal skin): note PAS positivity (purple) of cells and basal membrane. **B** (6 h after death): note PAS negativity (absence of purple) of cells compared to PAS positivity (purple) of basal membrane

Fig. 4 A, B Secretory cells (S-100 protein × 400). **A** (normal skin): note S-100 positivity (brown) of cells. **B** (12 h after death): note decrease in S-100 positivity (brown) of cells

Table 3 Alcian-PAS purple intensity during 12 h after death

	Purple intensity			
Cell type	0 h	3 h	6 h	9 and 12 h
Secretory cells	+++	+	–	–
Duct cells	+	–	–	–
Basal membrane	+++	+++	+++	+++

+++, Maximum stain intensity
++, Medium stain intensity
+, Minimum stain intensity

Table 4 S-100 positivity during 12 h after death

	S100-Protein positivity			
Cell type	0 h	3 h	6 h	9 and 12 h
Secretory cells	+++	+++	++	+
Duct cells	–	–	–	–
Basal membrane	–	–	–	–

+++, Maximum stain intensity
++, Medium stain intensity
+, Minimum stain intensity

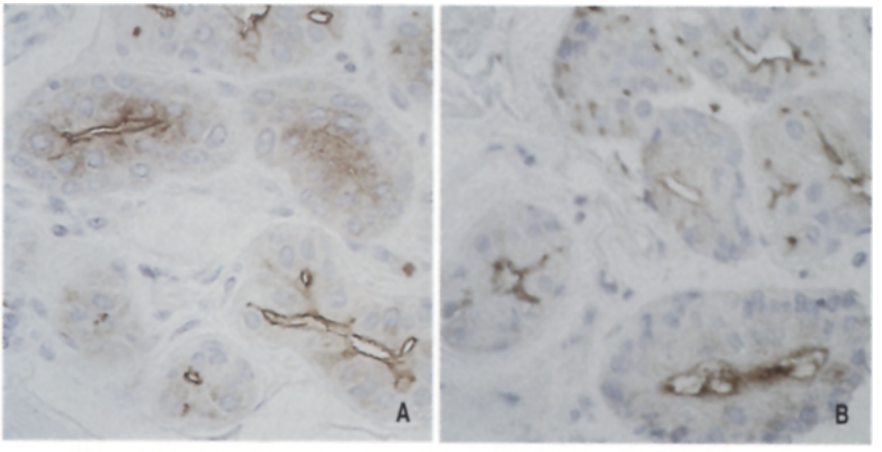

Fig. 5 A, B Secretory cells (CEA × 400). **A** (normal skin): note CEA positivity of lumen cell membrane (brown ring). **B** (12 h after death): note long-lasting CEA positivity of lumen cell membrane (*brown ring*)

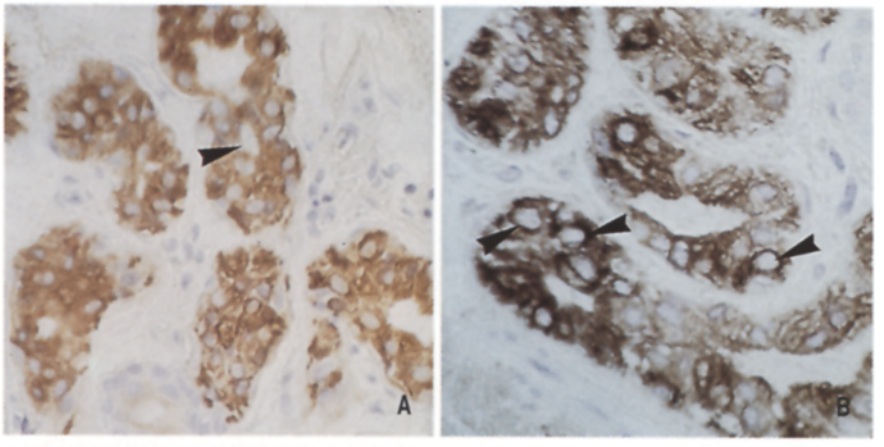

Fig. 6 A, B Secretory cells (Cytokeratin × 400). **A** (normal skin): note cytokeratin positivity (brown) of cells: **B** (12 h after death): note reduction in cellular stain (brown) and increase in cytoplasmic vacuoles (*arrows*) in cells

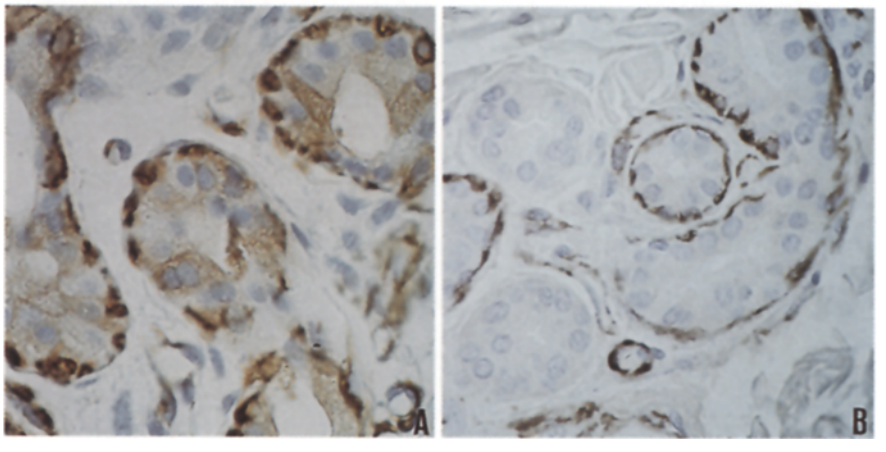

Fig. 7 A, B Myoepithelial cells (ASM × 400). **A** (normal skin): note strong ASM positivity (brown) of myoepithelial elements. **B** (12 h after death): note long-lasting ASM positivity (brown) of myoepithelial elements

Table 5 ASM positivity during 12 h after death

	S100-Protein positivity			
Cell type	0 h	3 h	6 h	9 and 12 h
Secretory cells	+++	+++	++	+
Duct cells	–	–	–	–
Basal membrane	–	–	–	–

+++, Maximum stain intensity
++, Medium stain intensity
+, Minimum stain intensity

Immunohistochemistry

The S-100 Protein test stains secretory tubule cells, especially the clear cells (Fig. 4A) which control the ion balance of secretory products. Variations in positive staining with time (Table 4 and Fig. 4B), only allow subjective determination of the time of death within the first 12 h.

The CEA test stains secretory cells which form a continuous ring round the lumen of the tubule and secretory capillaries (Fig. 5A), but no significant variations in staining positivity were observed with time after death (Fig. 5B).

The Cytokeratin test stains secretory tubule cells, especially clear cells (Fig. 6A), but no variations were observed after 3 h. With time, a progressive reduction in cell staining was observed, with an increasing number of "optical empty vacuoles" (Fig. 6B). The usefulness of this test is limited, because it gives the same morphological information as the hemotoxylin-eosin test.

The ASM test stains myoepithelial cells strongly and secretory cells weakly (Fig. 7A). The non-significant variations in staining positivity with time (Table 5 and Fig. 7B), confirm the structural resistance of smooth muscle cells to oxygen deficiency [13, 14], and limit the usefulness of this test.

Table 6 Time course variations in subcellular morphology of sweat glands

Time after death	Clear cells	Dark cells	Myoepithelial cells	Duct cells
3 h	– Strong reduction in intracellular glycogen (Fig. 8); – Initial mitochondrial dilatation, with slight rarefaction of cristae; – Appearance of lipofuscin granules; – Initial ER dilatation;	– Strong reduction in intracellular glycogen – Initial mitochondrial dilatation, with slight rarefaction of cristae; – Appearance of lipofuscin granules; – Reduction in number of secretory granules (Fig. 9);	– No evidence of morphological alteration in cytoplasmic organules;	– Mitochondrial dilatation;
6 h	– Evident mitochondrial dilatation, with rarefaction of cristae; – Increase in lipofuscin granules; – ER dilatation;	– Evident mitochondrial dilatation, with rarefaction of cristae (Fig. 10); – Presence of lipofuscin granules (Fig. 10); – ER dilatation;	– Morphological degeneration of cytoplasmic organules of outer parts of cells;	– Further mitochondrial dilatation;
9 h	– Further mitochondrial dilatation; – Difficult morphological characterisation of mitochondrial cristae; – Increase in lipofuscin granules; – Rarefaction of secretory capillary and luminal microvilli (Fig. 11);	– Further mitochondrial dilatation; – Difficult morphological characterisation of mitochondrial cristae; – Rarefaction of luminal cell membrane (Fig. 11);	– Initial ER dilatation; – Progressive degeneration of cytoplasmic organules of inner parts of cell;	– No variations;
12 h	– Dilatation of mitochondria, with disappearance of mitochondrial cristae; – Nuclear pyknosis; – Complete morphological degeneration of cytoplasmatic organules; – Dilatation of nucleus, with rupture of nuclear membrane; – Disappearance of secretory capillary microvilli.	– Dilatation of mitochondria, with disappearance of mitochondrial cristae; – Maximal ER dilatation; – Presence of immature secretory granules in ER;	– Cytoplasmic vacuolization; – Myofilament condensation; – Nuclear alterations;	– Mitochondrial dilatation; – Reduction in cell membrane interdigitation; – Dilatation of microvilli;

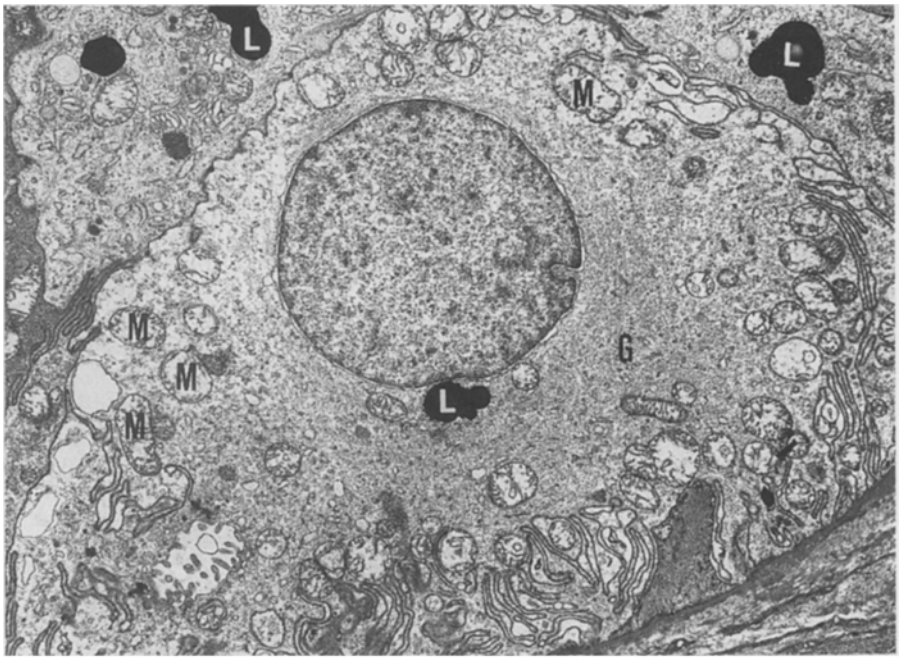

Fig. 8 Electron microscopy (× 10,000). Clear cell (3 h after death): note early mitochondrial (M) dilatation, great reduction in cytoplasmic glycogen granules (G) and early presence of lipofuscin granules (L)

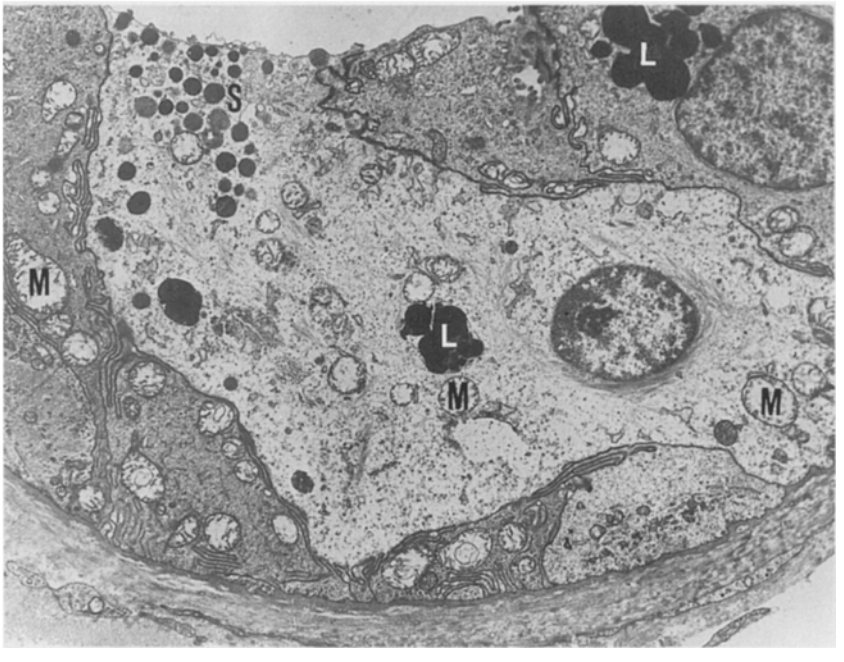

Fig. 9 Electron microscopy (× 10,000). Dark cell (3 h after death): note rarefaction of secretory granules (S), mitochondrial dilatation (M) and early presence of lipofuscin granules (L)

Electron microscopy

Variations in the subcellular morphology of sweat glands with time are reported in Table 6 and shown in Figs. 8–11. Electron microscopy allows cell types to be distinguished, together with morphological alterations of cell organules and parameters which change with time after death. Three hours after death secretory cells showed the most useful morphological alterations (Figs. 8 and 9). They appeared to be very sensitive to oxygen deficiency, as displayed by early mitochondrial dilatation and great reduction in the number of cytoplasmic glycogen particles. While determination of initial mitochondrial dilatation may be a subjective observation, this abnormality is typical of this stage and is easy to identify in clear cells. Another useful morphological alteration is rarefaction of secretory granules in dark cells (Fig. 9). These subcellular changes may help in determining the time of death within the first 3 h. No useful morphological variations occurred in duct or myoepithelial cells.

Six hours after death the most important parameters were the presence of dark lipofuscin granules in both clear and dark cells (Fig. 10). These granules were absent in other cell types. Extensive dilatation of mitochondria, to-

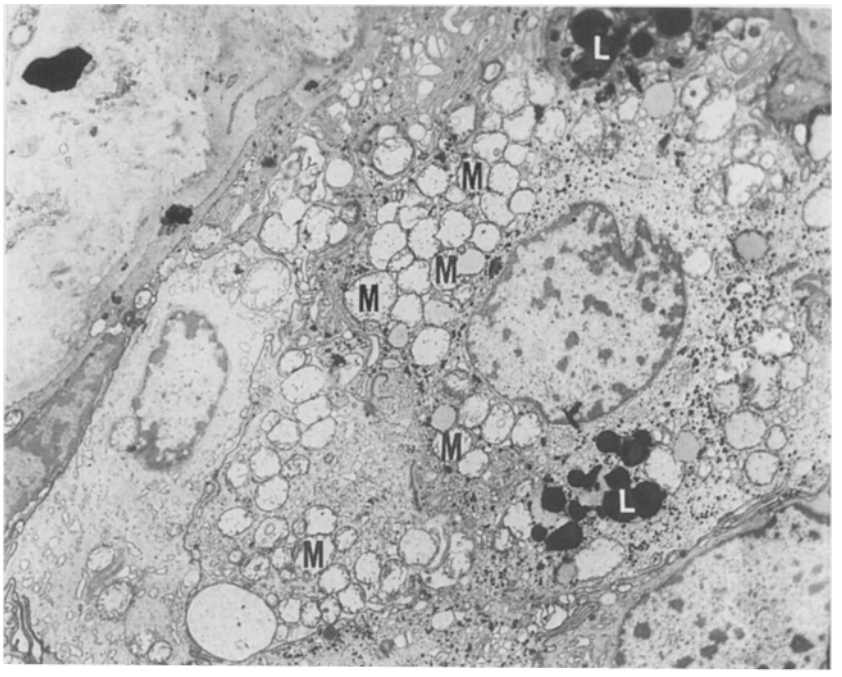

Fig. 10 Electron microscopy (× 10,000). Dark cell (6 h after death): note presence of lipofuscin granules (L) and great mitochondrial dilatation (M)

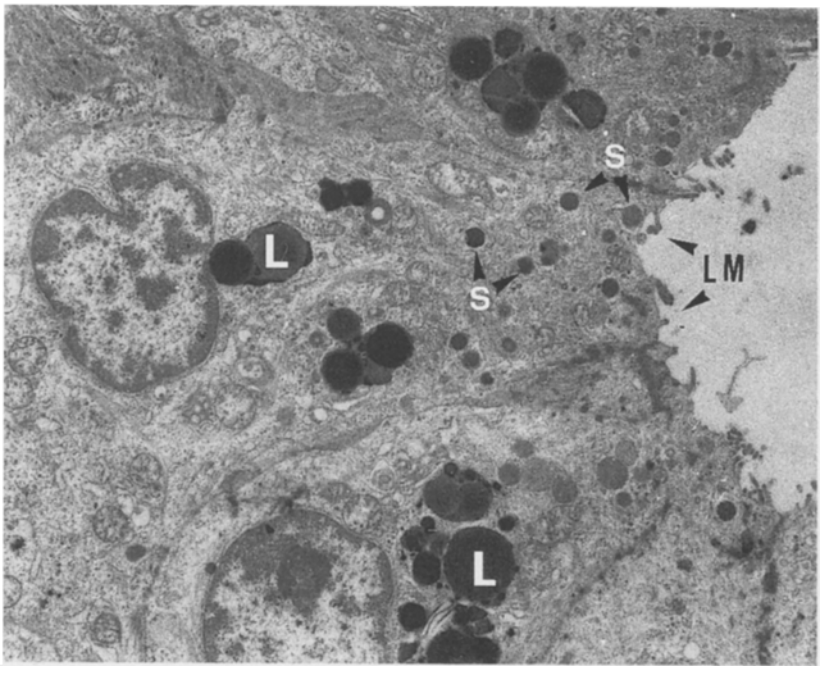

Fig. 11 Electron microscopy (× 10,000). Secretory cells (9 h after death): note rarefaction of lumen microvilli (LM), reduction of secretory granules (S), increase in lipofuscin granules (L) and mitochondrial alterations

gether with rarefaction of their cristae, also occurred at this time. This change now becomes useful because the enlargement and internal morphological alteration of these cytoplasmic organules were more evident than at 3 h. Degeneration of the cytoplasmic organules of the outer part of myoepithelial cells could not easily be observed. No other useful morphological variations in duct or myoepithelial cells could be observed.

Nine hours after death the most evident morphological alterations occurred in the cell membrane of secretory cells (Fig. 11), consisting of rupture of the cell membrane and rarefaction of cell membrane microvilli; such rarefaction between the clear cells was very typical. Furthermore, extensive morphological degeneration of cytoplasmic organules occurred in clear, dark and myoepithelial cells, particularly of the mitochondria (extensive enlargement and disappearance of cristae).

Twelve hours after death abnormalities in duct cells occurred, and mitochondrial dilatation, reduction of cell membrane interdigitation, dilatation of cell membrane microvilli, were all manifest.

Table 7 Potential for determining morphology of sweat glands and post-mortem intervals

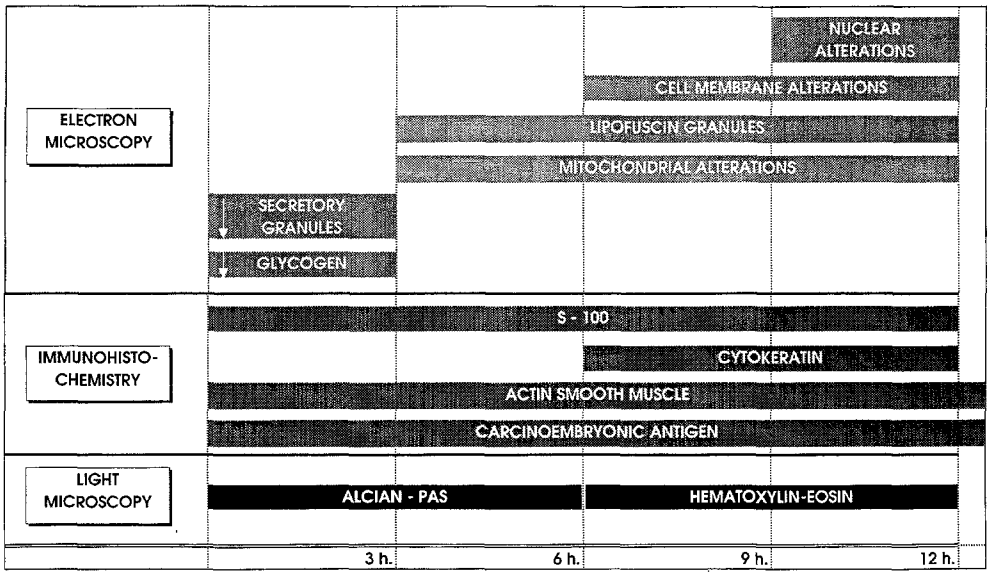

Conclusions

Table 7 summarizes the potential for determining post-mortem intervals by means of all the optical, electron microscope and immunohistochemical techniques used here to study eccrine sweat gland morphology.

The combined use of these techniques is proposed for further in-depth experimental studies on large numbers of samples, which may lead to their profitable use in forensic practice in the future.

References

1. Coe JI (1993) Postmortem chemistry update. Emphasis on forensic applications. Am J Forensic Med Pathol 14:91–117
2. Fisher RS (1980) Time of death and changes after death – Anatomical considerations. In: Spitz WU, Fisher RS (eds) Medicolegal investigation of death. Charles C Thomas, Springfield, pp 12–32
3. Janssen W (1984) Forensic histopathology. Springer, Berlin, pp 24–25
4. Balercia G, Cingolani M, Cinti S, Sabattani PG, Tagliabracci A (1986) Alterazioni ultrastrutturali postmortali della cute e cronologia della morte. Medicina Legale Oggi – Atti XXIX Congresso S. I.M.L.A. Cepi, Roma, p 21
5. Cangiotti AM, Morroni M, Tagliabracci A, Cingolani M (1986) Aspetti ultrastrutturali delle ghiandole sudoripare eccrine umane normali nel giovane e nell'anziano. Riv It Biol Med 6:148–151
6. Sato K (1977) The physiology, pharmacology and biochemistry of the eccrine sweat gland. Rev Physiol Biochem Pharmacol 79:51–129
7. Sato K, Sato F (1983) Individual variations in structure and function of human eccrine sweat gland. Am J Physiol 245: 203–208
8. Weiss L (1988) Cell and tissue biology. Urban & Schwarzenberg, Baltimore, pp 96–102
9. Sato K, Sato F (1990) Methods for studying eccrine sweat gland function in vivo and in vitro. Methods Enzymol 192: 583–587
10. Sterberger LA (1979) Immunocytochemistry. John Wiley, New York, pp 104–157
11. De Lellis RA (1981) Diagnostic immunohistochemistry. Masson, New York, pp 50–52
12. Bijman J (1987) Transport processes in the eccrine sweat gland. Kidney Int 32:109–112
13. Bernheim P, Willot M, Muller P (1966) Quelques aspects de l'autolyse du muscle strié humain au microscope optique et électronique. Ann Méd Lég 46:447–452
14. Suzuky T (1976) An ultramicroscopic study on rigor mortis. Forensic Sci Int 8:207–216